ISSN 1028-334X, Doklady Earth Sciences, 2024, Vol. 516, Part 2, pp. 1042–1049. © Pleiades Publishing, Ltd., 2024.
ISSN 1028-334X, Doklady Earth Sciences, 2024. © Pleiades Publishing, Ltd., 2024.

ATMOSPHERIC AND HYDROSPHERIC PHYSICS

Loading Effect of the Atmosphere on the Hydrosphere

Academician G. I. Dolgikh[a],* and M. A. Bolsunovskii[a]

Received January 29, 2024; revised February 14, 2024; accepted February 20, 2024

Abstract—By processing satellite data on the total electron content on a track between GLONASS, GPS, and ground receiving stations located in Primorsky Krai of Russia, disturbances of an electron layer with periods from 5 to 45 min, which are caused by natural atmospheric fluctuations, were identified. They affect the sea surface and are responsible for aquatic fluctuations with periods from 5 to 40 min.

Keywords: total electron content, satellite, natural fluctuations

DOI: 10.1134/S1028334X24601445

Study of the interaction of geospheric fields of various frequency ranges was extremely urgent and remains also topical at present. This is related to the determination of primary sources of these fields and, what is especially important, to the study of the physics of their origination and evolution. At the first stage of study of this interaction, it is important to determine the primary source of processes, fluctuations, and waves. These studies were conducted, and their results are published in numerous papers, e.g., [1, 2], in which it is stated that atmospheric fluctuations were responsible for fluctuations at the corresponding frequencies, as well as aquatic fluctuations in water, which were initially compared with inner shelf waters. More interesting results were acquired during the explanation of fluctuations registered by various marine stations in the Pacific Ocean after the explosion of Hunga Tonga—Hunga Ha'apai volcano. Some first published works stated that the sea level changes were caused by two types of tsunami waves generated by the explosion of this volcano [3]. The first tsunami waves were caused by natural oscillations of the atmosphere in the area of a level-measuring station, which were induced by the propagated explosion pulse, and the second ones included the tsunami waves resulting from the explosion. The first waves (meteotsunami) were objectively present in contrast to the second ones. This follows from (i) the fact that the propagation velocity of the disturbance from the explosion area to the registration area is approximately equal to the sound velocity in air and no other disturbances were registered by the level-measuring stations [4] and (ii) the spectral components at each level-measuring station were different and, probably, corresponded to the spectral components of natural fluctuations of atmospheric layers in the place of the location of stations [4].

This work presents challenges on the determination of the primary sources of fluctuations, which were registered by some level-measuring stations provided in [4], on the basis of the analysis of completely different experimental data of satellite monitoring. The pri-

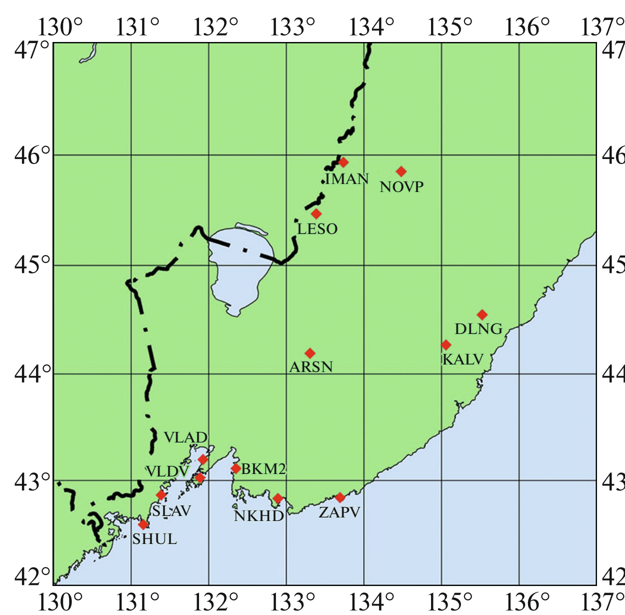

Fig. 1. Position of GNSS stations in Primorsky Krai. ARSN, Starosysoevka; BKM2, Mt. Bolshoi Kamen; DLNG, Dalnegorsk; IMAN, Dalnerechensk; KALV, Kavalerovo; LESO, Losezavodsk; NKHD, Nakhodka; NOVP, Novopokrovka; SHUL, Cape Shults; SLAV, Slavyanka; VLAD, Vladivostok; VLDV, Russkii Is.; ZAPV, Zapovednyi.

[a] *V.I. Il'ichev Pacific Oceanological Institute, Far Eastern Branch, Russian Academy of Sciences, Vladivostok, 690041 Russia*
**e-mail: dolgikh@poi.dvo.ru*

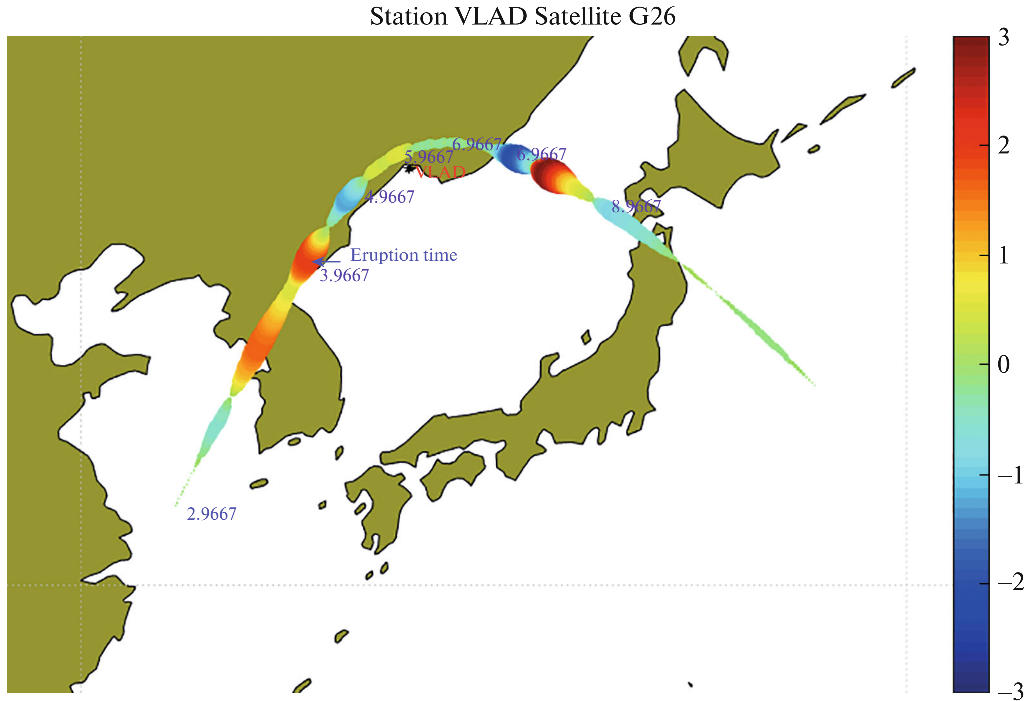

Fig. 2. Station–VLAD-G26 satellite track showing the position of the corresponding stations, time of response (hours UTC), and the color scale showing the TEC variations.

mary experimental data include data on the total electron content (TEC), i.e., the integral electron concentration, which characterizes the amount of free electrons in the entire thickness of the ionosphere on a track between the satellite and the surface receiving station. The height of maximum ionization on the day of eruption was ~300 km from the Earth's surface.

Note also a moderate geomagnetic storm shortly before the volcanic eruption, which caused disturbances in the Earth's ionosphere. The presence of the storm was identified using the geomagnetic index Kp, which is determined by stations in the middle latitudes and which characterizes the geomagnetic conditions on the planet [5].

During the analysis, we used the data on Global Navigation Satellite Systems (GNSS) from GLONASS satellite systems (24 satellites at heights of 18 840–19 440 km) and GPS (32 satellites at heights of ~20 150 km) by the following surface GNSS stations located in Primorsky Krai: ARSN, BKM2, DLNG, IMAN, KALV, LESO, NKHD, NOVP, SHUL, SLAV, VLAD, VLDV, and ZAPV (Fig. 1). Some stations are part of a complex geodynamic network of the Far East Branch, Russian Academy of Sciences [6]. The frequency of discretization of the GNSS data is 0.033(3) Hz. The TEC value was determined following [7, 8], and the precision of its determination by phase measurements is 0.01–0.02 TECU [9].

All satellites followed trajectories, the projections of which on Earth cross several territories and water basins. The receiving GNSS stations in Primorsky Krai registered the TEC of the layer located in the ionosphere. Taking into account that the heights of the satellites above the Earth's surface are 60–80 times higher than the height of this layer, we can consider that the data from a satellite–receiving GNSS station track would correspond to the ionospheric data of certain territories, above which these tracks occur. Figure 2 shows the receiving GNSS station–satellite VLAD-G26 track. It shows the position of the corresponding GNSS stations, the time of response (hour UTC), and the color scheme showing the TEC variations.

This figure indicates the TEC intensity of the ionosphere above a certain surface point. Figure 3a shows the area of TEC record in the ionosphere at the BKM2 station, when the satellite was visible for this station, and Fig. 3b shows its spectrum based on the periodogram method with averaging of 2. The spectrum contains powerful maxima on frequencies corresponding to periods of 39 min 23.1 s, 29 min 26.7 s, 17 min 39.3 s, 14 min 37.7 s, and 11 min 22.7 s. These data belong to the entire processing series.

We are also interested in areas of records that coincide with the position of some level-measuring stations described in [4] and shown in Fig. 4 (stations with numbers 8–15), i.e., those stations close to which the satellite–GNNS station tracks occur. The main results concern the ionospheric disturbances, which are located above/close to the level-measuring stations 13–15. Limited data are available on the ionospheric

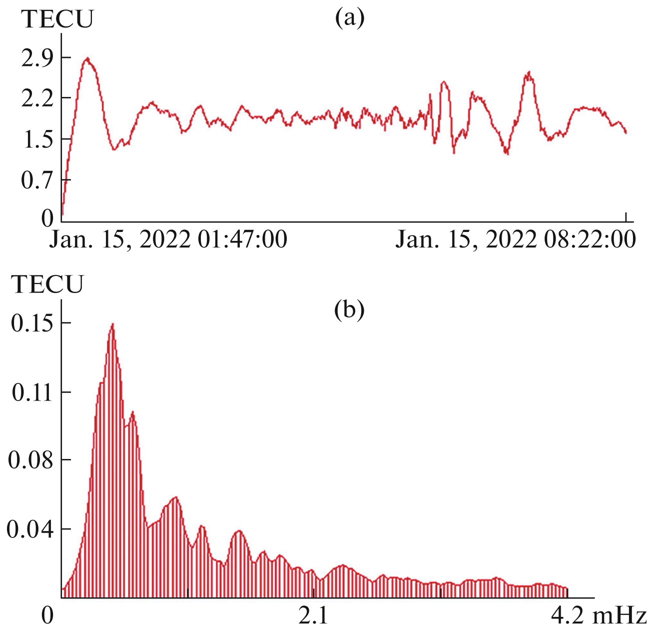

Fig. 3. Change in TEC during propagation of satellite G31 (a) registered by the BKM2 ground station and its spectrum (b).

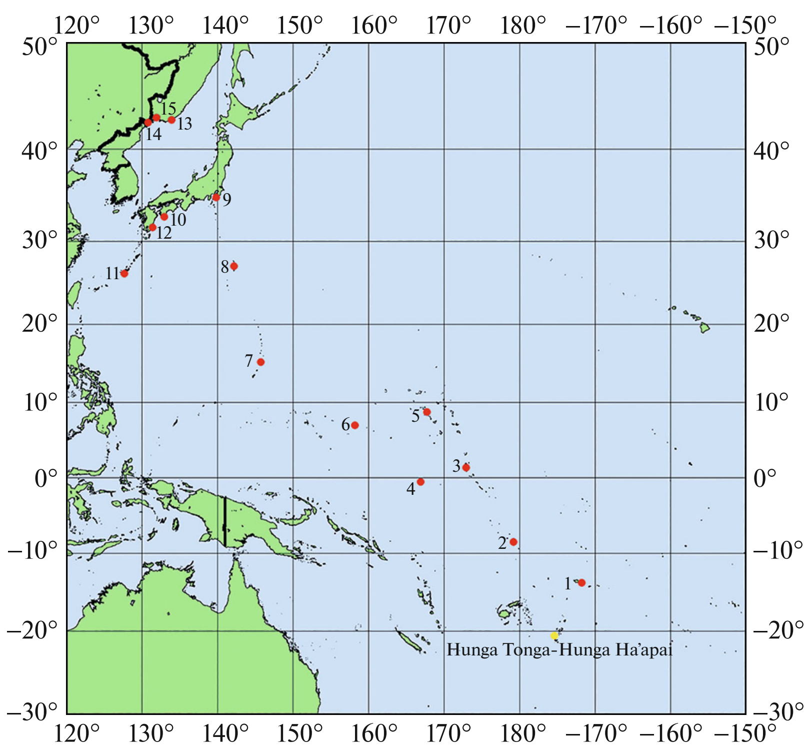

Fig. 4. (1–12) Stations located in the Pacific Ocean. The red circle marks the position of laser-interference receiving systems.

disturbances above/close to the level-measuring stations 9, 10, and 12. Only limited data are available on the ionospheric disturbances by level-measuring stations 8 and 11. No data are available on other level-measuring stations, because they occur beyond the registration possibilities of the receiving GNSS stations located in Primorsky Krai (Fig. 1).

Our experimental data on satellite–GNNS station tracks were divided into temporal sectors, the center of which was most closely located to the level-measuring

Table 1. Level-measuring stations

Station no.	Title	Periods Background [4]	Periods Signal [4]
8	Chichijima	20 min 28.0 s 16 min 30.3 s 13 min 49.7 s	20 min 28.0 s 15 min 02.9 s 12 min 47.5 s
9	Mera	6 min 09.9 s 5 min 19.8 s 22 min 14.7 s	22 min 14.7 s 6 min 05.5 s 6 min 38.7 s
10	Tosashimizu	20 min 28.0 s 39 min 21.4 s	20 min 28.0 s 24 min 21.8 s 42 min 38.2 s
11	Naha	26 min 55.7 s	24 min 21.8 s 10 min 26.5 s 22 min 14.7 s 25 min 34.9 s 19 min 40.7 s
12	Aburatsu	26 min 55.7 s 17 min 38.6 s 11 min 37.7 s	22 min 14.7 s 10 min 26.5 s 9 min 18.2 s
13	Preobrazheniye	31 min 58.7 s 15 min 59.3 s	30 min 05.8 s 9 min 28.5 s 15 min 59.3 s
14	Pos’et	31 min 58.7 s 17 min 38.6 s 10 min53.2 s	30 min 05.8 s 17 min 38.6 s 11 min 22.2 s
15	Vladivostok	39 min 21.4 s 31 min 58.7 s	31 min 58.7 s

stations shown in Fig. 4. Thus, each level-measuring station corresponded to a certain area of the experimental data. Further, these sectors were processed using the periodogram method, as well as the maximum likelihood method with the number of harmonics of 60 [10]. This number was chosen, because the duration of processed observation areas was mostly 128 points; i.e., the number of spectral components (harmonics) even during spectral processing by the Fourier fast transformation method will be 64.

We consider that the fluctuations of the water surface, which were registered at the explosion pulse propagation in the atmosphere [4], were caused by induced natural atmospheric fluctuations in the zone of the position of the given level-measuring station. In this paper, we suggest that the fluctuation periods of the electronic layer in the ionosphere, which occurs above the level-measuring station, are close to the fluctuation periods, which were registered by the level-measuring stations shown in [4]. For further analysis, Table 1 shows the experimental data (registered fluctuation periods) of the considered level-measuring stations published in [4].

Table 2 shows the maximum periods, which were distinguished after processing the areas of data on the TEC intensity in the ionosphere above the certain (or close) level-measuring station.

It follows from the comparison of data from Tables 1 and 2 that the maximum periods, which were distinguished from records of the level-measuring stations upon the atmospheric explosion pulse propagation, were close to those distinguished from records of TEC intensity of the ionospheric areas located above certain level-measuring station. This gives grounds to state that the primary source of these fluctuations is the same and is caused by natural fluctuations of certain atmospheric areas.

Table 2. Periods of maxima distinguished from processing of areas of TEC intensity in the ionosphere

Marine station no.	Ground station ARSN – satellite	Ground station BKM2 – satellite	Ground station KALV – satellite	Ground station SLAV – satellite	Ground station VLAD – satellite	Ground station SHUL – satellite	Ground station ZAPV – satellite	Ground station IMAN – satellite
8			**05:39–06:43** **R21** 14:03.2 18:17.7					
9	**07:04–08:09** **G31** 06:42.4	**07:18–08:22** **G31** 07:58.2	**06:43–7:47** **R21** 22:03.1 05:59.6	**06:39–08:48** **R11** 22:47.4 21:46.9	**05:40–09:57** **G26** 21:36.3	**09:38–10:44** **G16** 21:57.7	**05:36–10:17** **R21** 22:01.5 **06:40–08:49** **R21** 04:50.8 **22:11–23:16** **R21** 22:23.5 **06:31–09:54** **G26** 22:49.3	
10	**7:00–8:05** **R12** 19:57.7 **07:04–08:09** **G31** 41:23.4 20:15.9 **07:04–08:09** **G31** 20:15.9	**10:51–11:56** **R12** 19:06.2 **05:36–06:40** **G27** 39:56.6 **06:34–07:39** **G27** 44:22.5 **04:18–05:23** **G16** 44:22.5		**07:00–11:34** **R22** 42:43.0 **06:40–07:45** **R21** 24:42.5 **06:39–08:48** **R11** 41:39.6	**05:40–06:45** **R21** 20:29.9 **08:03–11:54** **R12** 38:36.6 **05:32–07:41** **G31** 19:41.4 **05:45–12:14** **G27** 43:11.5 21:24.7		**06:40–08:49** **R21** 43:21.2 **03:31–04:37** **G26** 41:56.0 19:02.1 **03:47–08:04** **G26** 19:09.6	**08:06–11:48** **R12** 42:38.2 **06:06–11:48** **R12** 42:14.6 **05:52–06:57** **G27** 19:50.2
11		**05:36–06:40** **G27** 19:08.9						
12		**05:36–06:40** **G27** 11:53.5c			**05:45–06:50** **G27** 22:21.6 10:17.5		**03:31–04:37** **G26** 21:59.5	
13	**09:09–10:13** **R22** 09:09.3 **07:07–09:15**	**07:51–08:56** **R12** 29:55.9	**05:46–06:51** **G16** 15:20.8 **10:03–11:08**	**06:40–07:45** **R21** 09:43.0 **05:36–10:20**	**07:26–08:24** **R22** 09:14.4 15:23.5	**04:32–05:37** **G26_1** 09:09.6 15:19.0	**22:11–23:16** **R21** 15:58.5 **06:49–07:54**	**07:36–11:59** **R22** 31:46.7 **05:52–12:18**

Table 2. (Contd.)

Marine station no.	Ground station ARSN – satellite	Ground station BKM2 – satellite	Ground station KALV – satellite	Ground station SLAV – satellite	Ground station VLAD – satellite	Ground station SHUL – satellite	Ground station ZAPV – satellite	Ground station IMAN – satellite
	R21 09:28.0 **08:20–11:31** **R12** 30:45.8 **06:07–07:13** **G27** 09:09.3 **07:00–09:09** **G26** 16:15.6 **09:00–10:05** **G08** 09:04.0		**G16** 30:51.3	**R21** 31:44.9 **07:38–08:44** **G16** 16:12.1	**05:40–06:45** **R21** 15:35.2 09:13.8 **05:39–10:14** **R21** 30:54.1 **22:15–23:42** **R21** 15:56.6 **05:32–07:41** **G31** 15:36.1 **06:33–08:42** **G16** 09:46.1 **10:20–11:26** **G16** 09:45.9	**05:32–06:37** **G26** 09:01.0 **06:42–07:47** **G16** 09:04.7	**R11** 09:09.0 **05:43–07:51** **G16** 30:35.4 09:03.6 09:49.5	**G27** 30:26.3 **11:37–13:46** **G08** 09:54.0
14	**06:03–07:07** **R21** 17:05:0 **08:20–10:29** **R12** 18:00.4 **08:20–11:31** **R12** 30:45.8 **07:08–08:13** **G08** 16:51.0 **08:00–09:05** **G08**	**09:56–11:00** **R22** 17:50.8 **09:52–10:56** **R22** 17:27.4 **07:51–10:00** **R12** 17:53.2 **04:32–06:41** **G31** 10:50.4 **06:34–07:39** **G27**	**05:46–06:51** **G16** 10:35.1 **06:46–07:51** **G16** 17:25.1	**05:36–10:20** **R21** 31:44.9 **03:32–04:37** **G26** 10:41.9 **04:32–05:37** **G26** 11:00.9	**07:26–11:44** **R22** 11:02.1 **06:44–07:49** **R21** 11:05.9 **22:15–23:20** **R21** 11:32.4 **08:03–10:12** **R12** 17:07.6 11:55.0 **06:45–08:54**	**03:32–04:35** **G26** 10:44.0	**04:32–06:41** **G26** 17:01.2 **05:43–07:51** **G16** 30:35.4 11:13.9	**07:36–11:59** **R22** 17:02.0 **05:52–12:18** **G27** 30:26.3 **06:57–08:01** **G08** 17:36.6

Table 2. (Contd.)

Marine station no.	Ground station ARSN – satellite	Ground station BKM2 – satellite	Ground station KALV – satellite	Ground station SLAV – satellite	Ground station VLAD – satellite	Ground station SHUL – satellite	Ground station ZAPV – satellite	Ground station IMAN – satellite
	30.09.4	17:11.6 11:23.0 **05:35–12:18** **G27** 17:21.3 11:49.7 **06:31–07:37** **G26** 17:40.1 10:26.0 **06:12–07:17** **G16** 11:07.3			**G27** 11:36.1 **05:45–12:14** **G27** 18:02.8 **05:40–09:57** **G26** 17:04.5 **10:20–11:26** **G16** 17:54.4			
15	**08:20–09:25** **R12** 39:44.7 29:35.9 **08:20–10:29** **R12** 41:29.9 **08:20–11:31** **R12** 40:44.4 **06:48–11:05** **G16** 40:01.1 32:32.0 **08:20–09:25** **R12** 29:35.9	**07:51–10:00** **R12** 40:02.6 **05:12–06:17** **G16** 39:38.8 10:56.4	**05:46–06:51** **G16** 39:33.0	**06:39–07:44** **G16** 30:51.3 31:28.6		**05:41–06:47** **G16** 29:39.2	**05:43–07:51** **G16** 30:35.4	**06:24–08:33** **G27** 31:31.4 **08:56–10:01** **G08** 31:59.1

FUNDING

This work was supported by the state contract “Study of Fundamental Basics of the Origination, Evolution, Transformation, and Interaction of Hydroacoustic, Hydrophysical, and Geophysical Fields of the World Ocean” (project no. AAAA-A20-120021990003-3) and the Federal Science Program “Substantiation of Climate Monitoring System of the Far Eastern Seas and Elaboration of Monitoring Methods of Extreme Weather–Climate Ocean-Related Events

Based on Stationary and Mobile Measurement Complexes and Multisensor Satellite Sounding."

ETHICS APPROVAL AND CONSENT TO PARTICIPATE

This work does not contain any studies involving human or animal subjects.

CONFLICT OF INTEREST

The authors of this work declare that they have no conflicts of interest.

REFERENCES

1. G. M. Shved, S. I. Ermolenko, N. V. Karpova, S. Wendt, and Ch. Jacobi, Izv., Phys. Solid Earth **49** (2), 278–289 (2013). https://doi.org/10.1134/S1069351313010138
2. G. I. Dolgikh, S. S. Budrin, S. G. Dolgikh, V. V. Ovcharenko, V. A. Chupin, V. A. Shvets, and S. V. Yakovenko, Dokl. Earth Sci. **462** (2), 631–634 (2015).
3. S. N. Kulichkov, I. P. Chunchuzov, O. E. Popov, G. I. Gorchakov, A. A. Mishenin, V. G. Perepelkin, G. A. Bush, A. I. Skorokhod, Yu. A. Vinogradov, E. G. Semutnikova, J. S. Epic, I. P. Medvedev, R. A. Gushchin, V. M. Kopeikin, I. B. Belikov, D. P. Gubanova, A. V. Karpov, and A. V. Tikhonov, Pure Appl. Geophys. **179**, 1533–1548 (2022). https://doi.org/10.1007/s00024-022-03046-4
4. G. Dolgikh, S. Dolgikh, and V. Ovcharenko, J. Mar. Sci. Eng. **10** (8), 1061 (2022). https://doi.org/10.3390/jmse10081061
5. Helmholtz Centre Potsdam. GFZ German Research Centre for Geosciences. https://www.gfz-potsdam.de/en/.
6. V. G. Bykov, N. V. Shestakov, M. D. Gerasimenko, A. A. Sorokin, A. V. Konovalov, A. S. Prytkov, N. F. Vasilenko, D. A. Safonov, A. G. Kolomiets, M. A. Serov, V. V. Pupatenko, S. P. Korolev, A. L. Verkhoturov, V. S. Zhizherin, and K. S. Ryabinkin, Vestn. Dal'nevost. Otd. Ross. Akad. Nauk, No. 3(211), 5–24 (2020). https://doi.org/10.37102/08697698.2020.211.3.001
7. E. Astafyeva, Rev. Geophys. **57**, 1265–1288 (2019). https://doi.org/10.1029/2019RG000668
8. B. Hofmann-Wellenhof, H. Lichtenegger, and E. Wasle, *GNSS-Global Navigation Satellite Systems,* 1st ed. (Springer, Vienna, 2008).
9. A. Coster, J. Williams, A. Weatherwax, W. Rideout, and D. Herne, Radio Sci. **48**, 190–196 (2013). https://doi.org/10.1002/rds.20011
10. A. A. Mitsel', *Applied Mathematical Statistics. Student's Book* (Tomsk State Univ. of Control Systems and Radioelectronics, Tomsk, 2022) [in Russian].

Translated by I. Melekestseva